



The Aerodynamic Performance of the Small-Scale Wind Turbine Blade with NACA0012 Airfoil

Siti Amni Husna Roslan¹, Zainudin A. Rasid^{1,*}, Ahmad Kamal Arifin Mohd Ehsan²

¹ Department of Mechanical Precision Engineering, Malaysia-Japan International Institute of Technology, Universiti Teknologi Malaysia, 54100 Kuala Lumpur, Malaysia

² Dept of Mechanical & Manufacturing Engineering, Faculty of Engineering and Built Environment, Universiti Kebangsaan Malaysia, 43600 Bangi, Selangor, Malaysia

ARTICLE INFO

Article history:

Received 12 August 2022

Received in revised form 5 September 2022

Accepted 27 September 2022

Available online 31 October 2022

Keywords:

small scale wind turbine; blade element momentum theory (BEMT); NACA0012; low Reynold's number condition

ABSTRACT

Small-scale wind turbine (SSWT) has been the subject of intensive research to complement its large-scale counterpart especially for usage in low wind speed regions. Two important issues that plague the development of the SSWT are its low in power coefficient especially due to the low Reynold's number (Re) condition that it's operating in and the start-up difficulty that it faces. In this paper, the blade element momentum theory (BEMT) has been used to analyse a small-scale wind turbine having 3 m diameter. The airfoil used is the NACA 0012. The simplified experimental based equations have been used to determine the coefficient of lift, C_L and coefficient of drag, C_D of the airfoil. A developed MATLAB's code applying the basic BEMT method is used. The results of aerodynamic performances including power coefficient, power and thrust are given as a function of wind speed, tip speed ratio (TSR) and Reynold's number. It shows that at the minimum wind speed of 3 m/s, the wind turbine can have power coefficient of 43% but to produce 600 W of power that is required for total needs of electrical consumption of a household, the wind speed needed is 5m/s which is reachable for low wind speed region.

1. Introduction

The high usage of carbon-based energy sources such as oil, gas and coal has caused the release of greenhouse gases and the climate crisis [1-3]. Other than solar energy, wind energy has been the choice of many countries to replace the conventional energy sources due to its green and sustainable nature [4-6]. To produce the wind energy, SSWT is catching up its large-scale counterpart especially in low wind speed regions and remote and even urban areas [7]. Even though the design of the small-scale wind turbine uses the same tools as for the large-scale wind turbine, 3 important criteria that characterize the small-scale wind turbine are its low Reynold's number (Re) condition, low start-up capabilities and low cost [8]. With low wind speed and small blade size, the wind flow operates at low Re that is dominated by drag, only to lower the wind turbine power coefficient, C_p [9-11]. Again,

* Corresponding author.

E-mail address: arzainudin.kl@utm.my (Zainudin A. Rasid)

with low wind speed, the start-up difficulties of the wind turbine need to be addressed in order to increase the annual energy production (AEP) [12]. Furthermore, the blade needs to be designed without most of the control systems available in its large counterpart in order to reduce cost. With these difficulties, the design of SSWT that nonetheless produces high power coefficient and capable of self-starting in lesser time without high installation cost is a challenge particularly to bring the SSWT to become competitive with its large-scale counterparts. Studies showed that the use of the SSWTs in the city of Shahrababak in Iran with powers of 300W, 600W or 1000W may be enough to cater the electrical consumptions of individual homes depending also on the yearly wind condition of the region [13, 14]. Furthermore, the average consumption per household in a South-East Asian country, Malaysia was found to be 345 kWh [15], where taking 15 hr./day average of power consumption, the required power for the SSWT is about 800 W.

The aerodynamic performances of airfoils have been studied using numerical methods and the BEMT [16]. Through the BEMT, shape optimization of the blades was conducted to determine the dimensions of the blade, torque, thrust, power coefficient and power of the wind turbine. Canale *et al.*, [17] compared 3 airfoils and the Joukowski airfoil was found to have good efficiency and shorter length for easier starting. The BEMT as well as experiments were used to study aerodynamic characteristics of BW3, A18 and SG6043 airfoils at low wind speed region in the UAE [18]. The BW3 airfoil was found to give the best $C_p=38\%$ at design wind speed of 5 m/s and tip speed ratio (TSR), $\lambda = 4.4$. The effect of twisting and tapering of the blade in the shape optimization process on the aerodynamic performances of the wind turbine was studied by Lee *et al.*, [19] using the BEMT. The effect of twisting and tapering gave 50% improvement of the C_p if compared to non-twisting and non-tapering blade. Similarly, in a study by Hsiao *et al.*, [20], the shape optimization of blades having NACA 4418 airfoil using the extended BEMT method was found to give the highest C_p .

In this study, the aerodynamic performances including the power coefficient, power and thrust of a small-scale wind turbine with NACA 0012 airfoil are determined using the BEMT method. The coefficient of lift, C_L and coefficient of drag, C_D of the airfoil are determined using simplified equations derived through results of experimental procedures conducted on the blade with the same airfoil [21]. MATLAB's codes developed by Wood [22], applying the BEMT method and the shape optimization process have been used in this study. The results of the aerodynamic performances are given as functions of wind speed, V , λ and Re .

2. Methodology

In this study, the aerodynamic performances of a wind turbine applying the NACA 0012 airfoil are determined. The performances here include the power coefficient, C_p , power, P , torque, T and thrust, F_a . The wind speed is varied between 3-11 m/s while the TSR used is between 1-15. The rotor diameter is 3 m which puts the wind turbine under the category of small-scale wind turbine. The specifications of the wind turbine are given in Table 1 while an example of the wind turbine used in this study is shown in Figure 1.

Table 1
The wind turbine specifications

Airfoil	NACA0012
Wind speed, V	3-11 m/s
Rotor diameter	3 m
No of blade	2
No of element	15
Tip speed ratio, λ	1-15



Fig. 1. A 3-bladed SSWT wind turbine [23]

2.1 The Airfoil

Figure 2 shows the NACA 0012 airfoil used in this study. This airfoil has been previously used in several studies [24, 25]. It is one of the earliest airfoils that applied no chamber in its design.

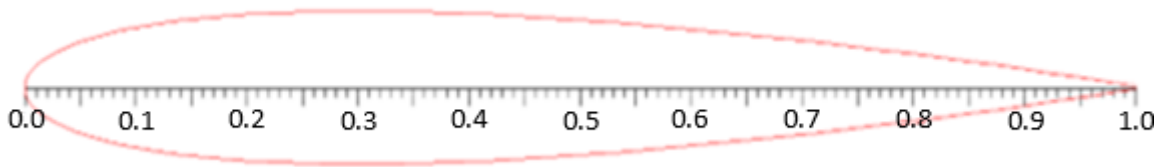


Fig. 2. The NACA0012 airfoil

For simplification purpose, in this study on the aerodynamic performances of a wind turbine, the C_L and C_D of the NACA 0012 airfoil are approximated through correlation formulae made through data taken from wind-tunnel experimental study [22, 24]. Such polynomials of the correlations are shown in Eq. (1) and Eq. (2) where it is apparent that C_L and C_D depend on α and Re only.

$$C_L = \alpha(0.1025 + 0.00485\log_{10}(Re/10^6)) \quad (1)$$

$$C_D = 0.004 + 0.018Re(10^{-0.15}) + 0.009(C_L/1.2)^2 \quad (2)$$

For the purpose of understanding the effect of α and Re on the C_L , C_D and the C_L to C_D ratio or known as the gliding ratio, L/D , the XFOIL codes have been used to determine the C_L , C_D and the L/D ratio. Figure 3 shows the plots of C_L and L/D ratio over angle of attack (AOA), α for several values of Re . The figure shows that the L/D ratio that is increased with Re where stall occurs in a more stable manner for over a range of angle of attack. Furthermore, the critical angle, α_{cr} can be seen to occur not at the maximum values of C_L . Table 2 shows the maximum C_L and L/D and their corresponding AOA for each Re .

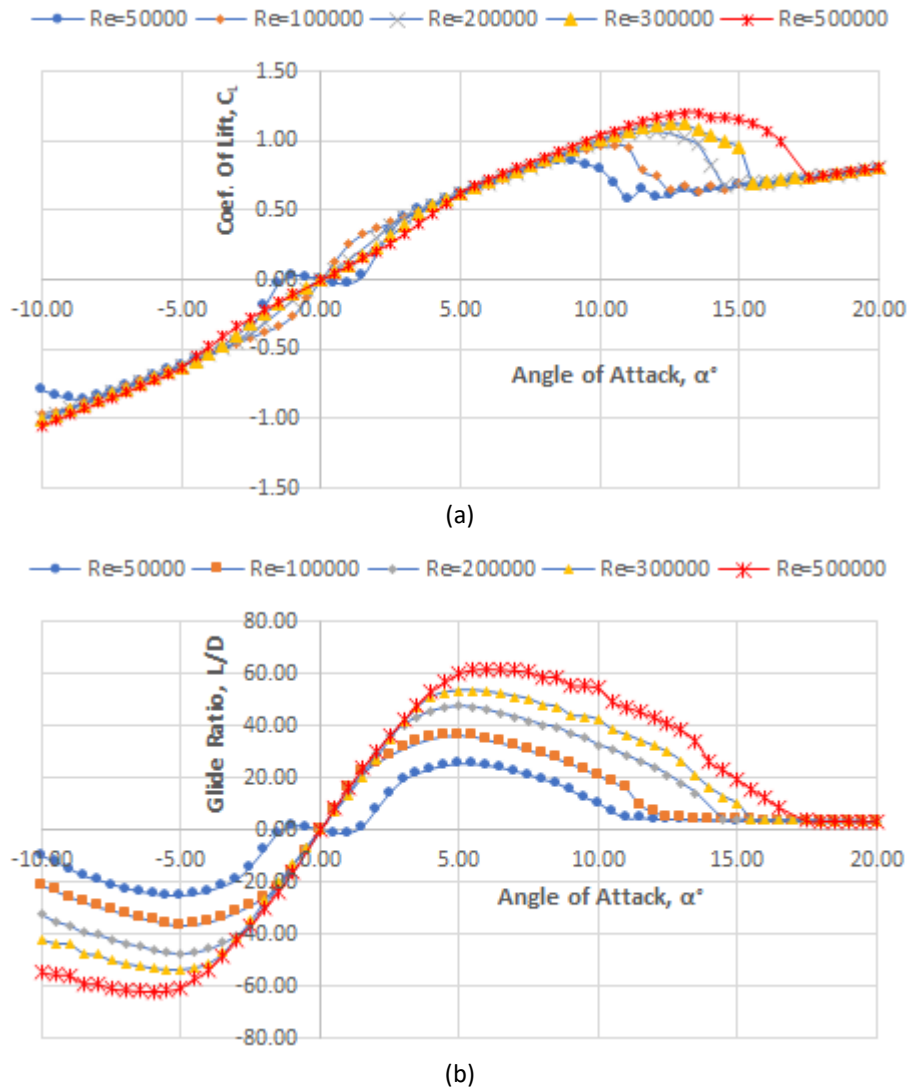


Fig. 3. The plots of (a) C_L and (b) L/D against AOA, α°

Table 2

The maximum C_L and L/D with its corresponding α for different Re s

Reynold's number	$C_{L,max}$ @ α	L/D_{max} @ α
50000	0.86 @ 8.5°	25.44 @ 5°
100000	0.97 @ 10°	36.61 @ 5°
200000	1.08 @ 12°	47.43 @ 5°
300000	1.13 @ 12.5°	53.54 @ 6.5°
500000	1.21 @ 13.5°	61.88 @ 6°

2.2 The Blade Geometry

As the requirement of the BEMT, the prepared geometry of the blade *i.e.*, the chord length and the twist angle for each element of the blades are as shown in Table 3. The values of the chord length and the twist angle were converted to polynomial forms of equations by Anderson [21, 22] which are used in this study.

Table 3
The blade chord length and twist

Radius (cm)	Chord length (mm)	Twist angle (°)
13.33	25.02	24.21
23.25	23.18	21.06
29.75	19.98	15.87
36.25	17.32	11.92
42.75	15.12	8.96
49.25	13.33	6.77
55.75	11.86	5.18
62.25	10.67	4.02
68.75	9.71	3.16
75.25	8.92	2.49
81.75	8.26	1.93
88.25	7.71	1.44
94.75	7.23	0.99
101.25	6.8	0.59
107.75	6.41	0.25
114.25	6.04	-0.06
120.75	5.7	-0.36
127.25	5.38	-0.67
133.75	5.08	-0.98
140.25	4.84	-1.28
146.75	4.66	-1.59
150	4.6	-1.74

2.3 The BEMT Analysis

In the BEMT analysis, the blade is divided into 15 elements where the analysis is required to find power and power coefficient for each element through an iteration process. The V and λ need to be input, following the values in Table 1. Referring to the flow-chart in Figure 4, with assumed values of initial axial and radial induction factor, a and a' respectively, the flow angle, ϕ and the angle of attack, α for each blade element can be calculated.

$$\phi = \frac{1 - a}{\lambda_r(1 + a')} \quad (3)$$

$$\alpha = \phi - \theta \quad (4)$$

The relative wind speed, can then be calculated along with the Reynold's number, Re .

$$V_{rel} = \sqrt{(1 - a)^2 + ((1 + a')\lambda_r)^2} \quad (5)$$

$$Re = \frac{V_{rel} * c * R}{\nu} \quad (6)$$

With the obtained values of Re and α , the values of C_L and C_D can be determined using Eq. (1) and Eq. (2). The thrust coefficient, C_a and torque coefficient, $C_{a'}$ can be calculated such as:

$$C_a = C_L \cos\phi + C_D \sin\phi \quad (7)$$

$$C_{a'} = C_L \sin \phi - C_D \cos \phi \quad (8)$$

Finding new induction factors, a_n and a_n' and defining solidity, $\sigma = \frac{Bc}{2\pi r}$ that represents the geometry of the blade, f_a is set as:

$$f_a = \frac{V_{rel}^2 \sigma C_a}{4V^2} \quad (9)$$

where B is the number of blades. Applying Glauerte's empirical correction when $a > 0.5$,

$$a_n = \begin{cases} \frac{(1+\sqrt{f_a-1})}{2} & f_a > 1 \\ \frac{(1-\sqrt{f_a-1})}{2} & f_a \leq 1 \end{cases} \quad (10)$$

The actual new a is taken as the average between the old, a and new, a_n .

$$a = \frac{a + a_n}{2} \quad (11)$$

and the radial induction factor,

$$a' = \frac{a C_{a'}}{C_a \lambda_r} \quad (12)$$

The thrust and torque for each blade element can be calculated such as:

$$dF_a = \frac{1}{2} \rho V_{rel}^2 c(r) N C_a dr \quad (13)$$

$$dT = \frac{1}{2} \rho V_{rel}^2 c(r) N C_{a'} r dr \quad (14)$$

The iteration continues until the difference between successive a and a' is within a specified tolerance of 0.0001. After adding the thrust and axial force for each blade element, the total thrust and torque are known.

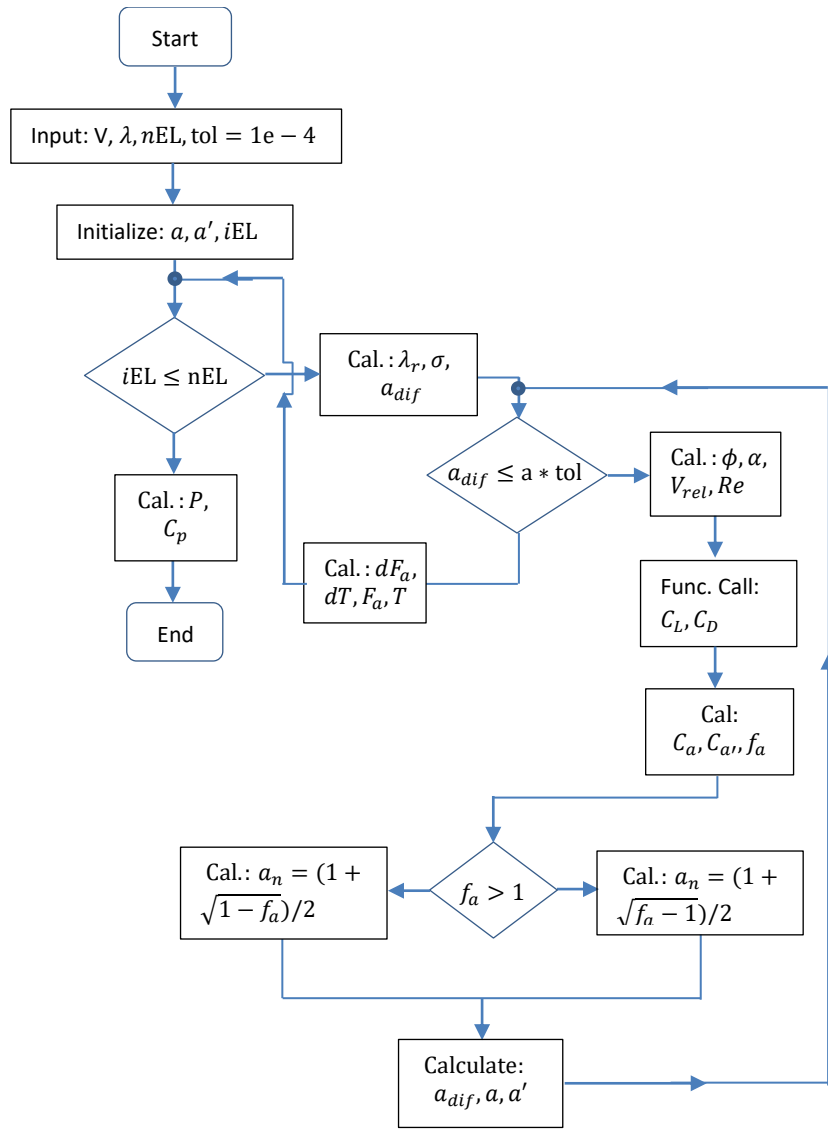


Fig. 4. The flow-chart for the BEMT analysis

Thus, power coefficient and power are:

$$C_p = T\lambda \tag{15}$$

$$P = \frac{1}{2}\rho AV^3 C_p \tag{16}$$

where ρ is air density and A is swept area of the blade. The BEMT here is solved through a developed MATLAB's codes [22] and the flow-chart for the codes applied in this study is given in Figure 4.

3. Results

3.1 Code's Validation

The results of the MATLAB's codes in this study are validated with experimental findings obtained by Anderson [21] where a 2-bladed wind turbine with NACA 0012 airfoil was used. The rotor diameter

was 3 m. Figure 5 shows that the results obtained in this study are closed to the experimental results where maximum power coefficient occurs in between 10-11 values of TSR.

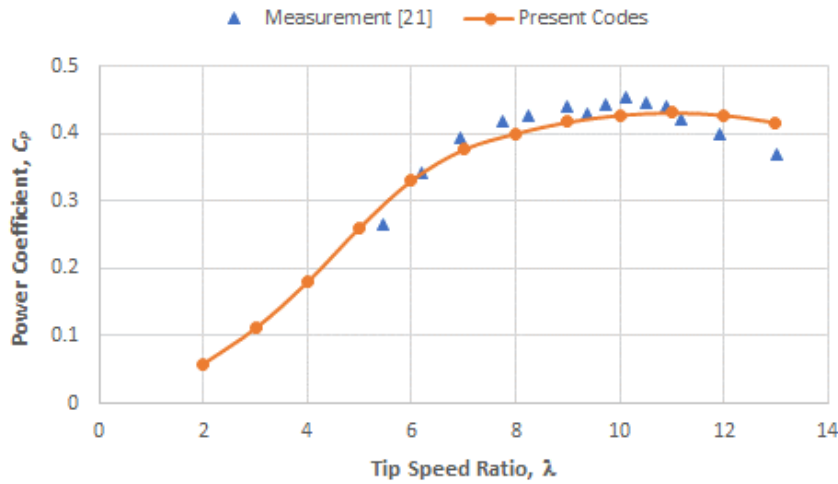


Fig. 5. The power coefficient, C_p vs TSR for several wind speeds

3.2 Power Coefficient

The power coefficient is plotted over a range of TSR and wind speed such as shown in Figure 6. The plots of C_p for all wind speeds are almost the same. This is probably due to the simplified assumptions made in this BEMT analysis. The plots show that as TSR is increased, C_p goes to increase as well until TSR is 11 when the C_p starts to decline. The maximum C_p for wind speed, $V = 3\text{m/s}$ is $C_p = 43\%$ at $\lambda_{max} = 11$. The trend of these plots is actually common as can be seen in a past literature [19, 26, 27].

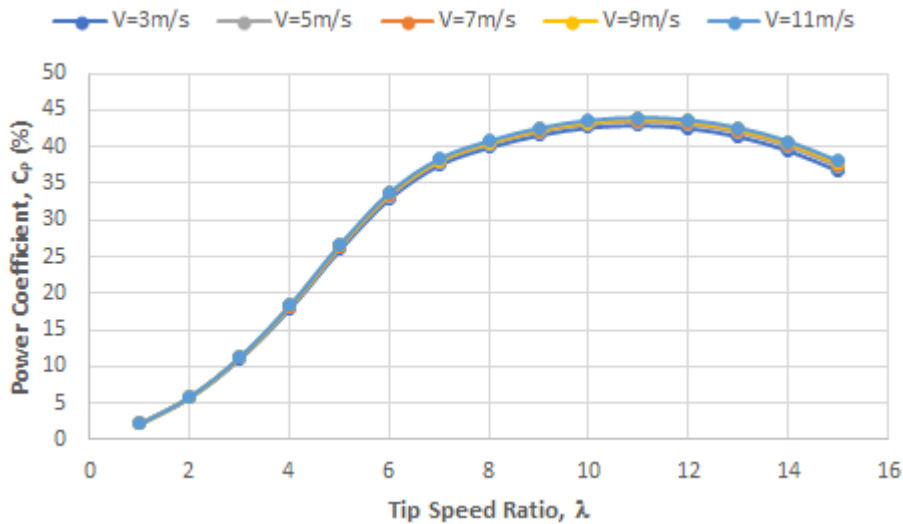


Fig. 6. The power coefficient, C_p vs TSR for several wind speeds

3.3 The Power

The plots of power, P against TSR for several wind speeds are shown in Figure 7. The plots show the same trend as the plots for power coefficient where maximum power occurs at TSR = 11. Table 4 shows the maximum power obtained for different wind speeds. It shows that at the mere speed of

$V=3$ m/s, power of 196.74 W can be obtained at TSR, $\lambda=11$. With studies showed that power of 600 W is enough for electrical requirement of a household [10, 11], using the NACA0012 airfoil can fulfil this condition at the wind speed of 5 m/s which is possible to obtain in low wind speed regions.

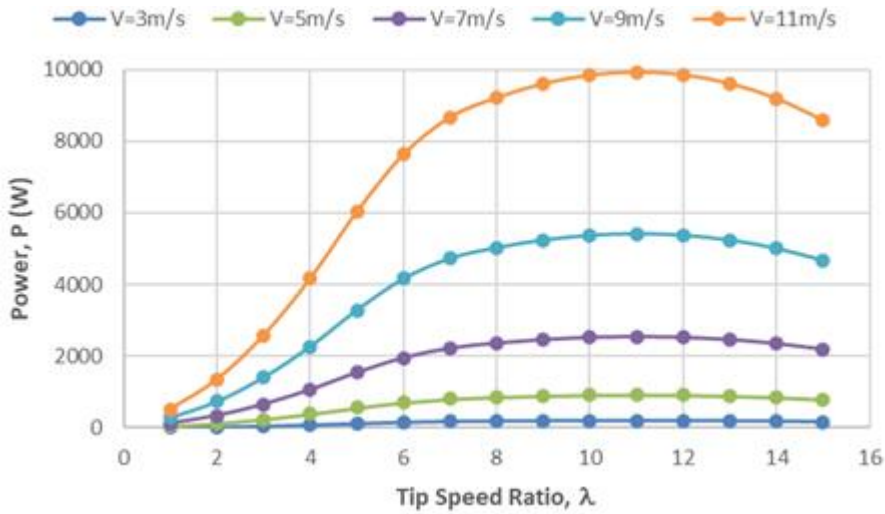


Fig. 7. The power, P vs TSR for several wind speeds

Table 4
 The maximum power for different wind speed

Wind Speed (m/s)	Maximum Power (W)	TSR
3	196.74	11
5	919.5	11
7	2538.21	11
9	5417.93	11
11	9925.28	11

3.4 The Thrust Force

Figure 8 shows the plot of thrust against TSR for different wind speeds. It shows the trend of nonlinear increase of thrust with increasing TSR but with no maximum thrust point. The thrust can also be seen to increase greatly with the increase of wind speed. At the TSR of $\lambda=6$, the thrust for wind speed, $V = 5$ m/s has increased by 180% if compared to the thrust for wind speed of $V = 3$ m/s.

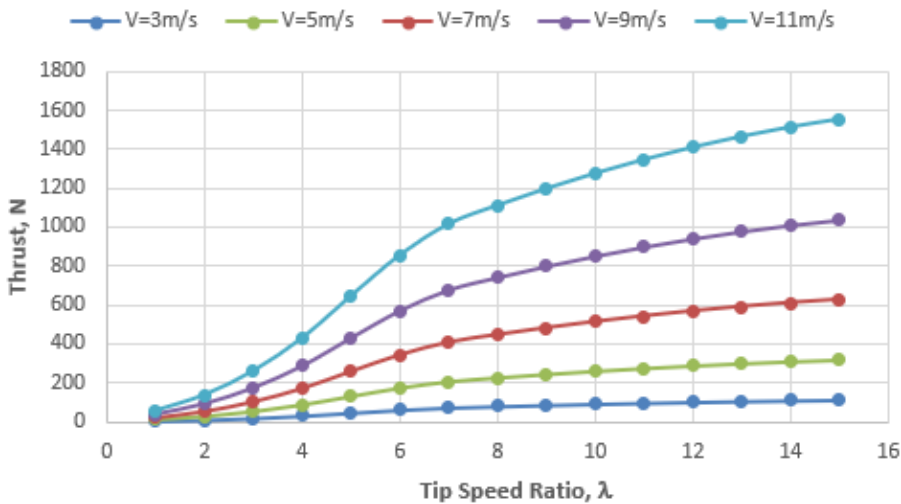


Fig. 8. The thrust, F_a against TSR for several wind speeds

The increase of thrust force with speed is related to the increase of Re at increasing wind speed. At low Re, flow is laminar with the occurrence of flow separation bubble. As such, lift force is lowered while drag force is increased. The torque as well as thrust will be decreased even though the latter is reduced at lower rate as described in Figure 9. The value of thrust force is important because this force is transmitted to the wind turbine tower. As such, the thrust force value is important in the design of the tower and its foundation. Furthermore, the thrust force also causes the deflection of the blade's tip where deformation above a limit is considered a failure. A study by Yang *et al.*, [2] was conducted to minimize the thrust other than maximize the torque.

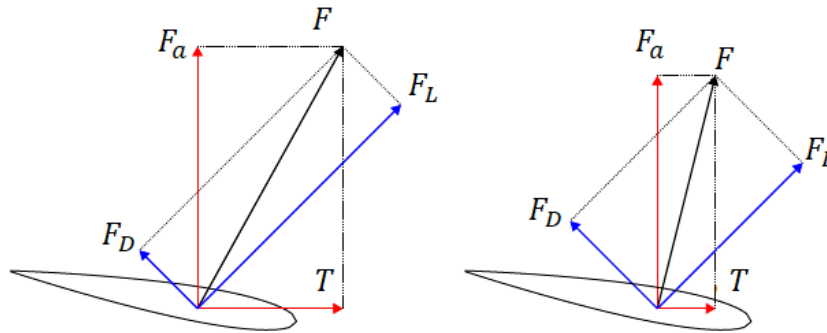


Fig. 9. The thrust, F_a against TSR for several wind speeds

3.5 The Effect of Reynold's Number

The Re is known to increase with the increase of wind speed where low Re at low wind speed has been the big reason that causes the lowered C_p of the wind turbine [28, 29]. Figure 10 shows the plots of power coefficients against Re for different wind speeds. The Re here corresponds to Re at the root of the blade that is increased as the TSR is increased. The plots show that as the wind speed increases, the Re is increased as well. As such, the C_p plots shifted to the right. At each wind speed, the C_p is increased to a maximum value as the Re is increased due to the increased in the TSR.

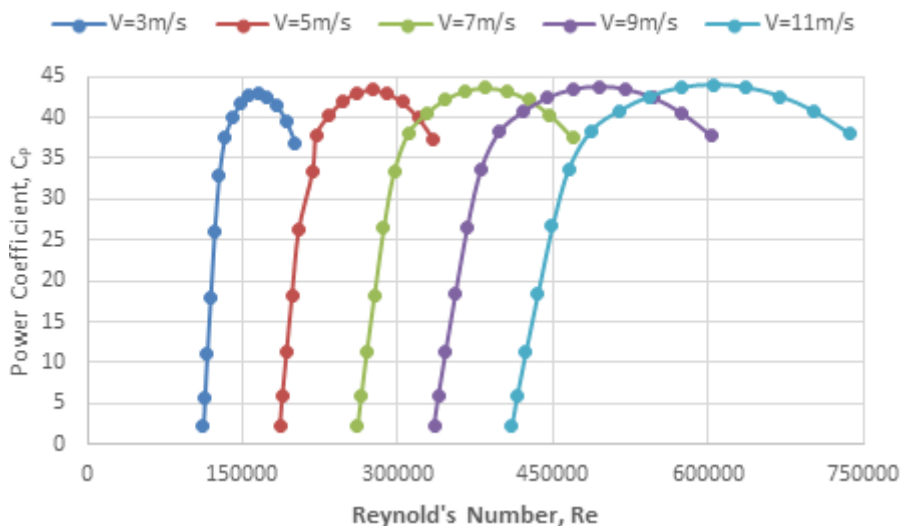


Fig. 10. The C_p against the Re for different wind speeds

4. Conclusions

The aerodynamic performances of a small-scaled horizontal wind turbine applying the NACA 0012 airfoil has been studied using the blade element momentum theory. The plots of power coefficient, power and thrust are found to have the similar trends with blades applying different airfoils observed from literatures where the values are increased with TSR and wind speed. While the power and power coefficient values give the main required values in the design of a wind turbine, the thrust force values are required in avoiding failures of blade, tower and its foundation. A rather high-power coefficient of about 43% at even the low wind speed of $V=3$ m/s can be obtained. However, to get the minimum requirement of 600 W for sufficient electrical application requirement of a household requires the wind speed of at least 5 m/s. This is obtainable in the low wind speed region through the use of diffuser that can increase the wind speed that enters the rotor of the wind turbine.

Acknowledgement

The authors acknowledge the support by the Faculty of Malaysia-Japan Institute of Technology, Universiti Teknologi Malaysia, Kuala Lumpur for providing the UTMER Scheme grant "Q.K.130000.2656.18J24".

References

- [1] RA Ghazalla, MH Mohamed, and AA Hafiz. "Synergistic analysis of a Darrieus wind turbine using computational fluid dynamics." *Energy* 189 (2019): 116214. <https://doi.org/10.1016/j.energy.2019.116214>
- [2] Han Yang, Jin Chen, Xiaoping Pang, and Gang Chen. "A new aero-structural optimization method for wind turbine blades used in low wind speed areas." *Composite Structures* 207 (2019): 446-459. <https://doi.org/10.1016/j.compstruct.2018.09.050>
- [3] K Rajendra Prasad, V Manoj Kumar, G Swaminathan, and Ganesh Babu Loganathan. "Computational investigation and design optimization of a duct augmented wind turbine (DAWT)." *Materials Today: Proceedings* 22 (2020): 1186-1191. <https://doi.org/10.1016/j.matpr.2019.12.116>
- [4] Khattak, M. A., NS Mohd Ali, NH Zainal Abidin, N. S. Azhar, and M. H. Omar. "Common Type of Turbines in Power Plant: A Review." *Journal of Advanced Research in Applied Sciences and Engineering Technology* 3, no. 1 (2016): 77-100.
- [5] Mondal, Mithun, Djamel Hissein Didane, Alhadj Hisseine Issaka Ali, and Bukhari Manshoor. "Wind Energy Assessment as a Source of Power Generation in Bangladesh." *Journal of Advanced Research in Applied Sciences and Engineering Technology* 26, no. 3 (2022): 16-22. <https://doi.org/10.37934/araset.26.3.1622>
- [6] Venkatramakrishnan, Sri Ragunath, Jitendra K. Pandey, Amit Kumar Mondal, and Ashish Karn. "Low Speed Wind Turbines for Power Generation: A Review." *Journal of Advanced Research in Fluid Mechanics and Thermal Sciences* 67, no. 1 (2020): 146-169.
- [7] Abhishiktha Tummala, Ratna Kishore Velamati, Dipankur Kumar Sinha, V Indraja, and V Hari Krishna. "A review on small scale wind turbines." *Renewable and Sustainable Energy Reviews* 56 (2016): 1351-1371. <https://doi.org/10.1016/j.rser.2015.12.027>
- [8] Abolfazl Pourrajabian. "Effect of blade profile on the external/internal geometry of a small horizontal axis wind turbine solid/hollow blade." *Sustainable Energy Technologies and Assessments* 51 (2022): 101918. <https://doi.org/10.1016/j.seta.2021.101918>
- [9] Md Robiul Islam, Labid Bin Bashar, Dip Kumar Saha, and Nazmus Sowad Rafi. "Comparison and Selection of Airfoils for Small Wind Turbine between NACA and NREL's S series Airfoil Families." *International Journal of Research in Electrical, Electronics and Communication Engineering* 4, no. 2 (2019): 1-11.
- [10] Ronit K Singh, M Rafiuddin Ahmed, Mohammad Asid Zullah, and Young-Ho Lee. "Design of a low Reynolds number airfoil for small horizontal axis wind turbines." *Renewable energy* 42 (2012): 66-76. <https://doi.org/10.1016/j.renene.2011.09.014>
- [11] Giguere, Philippe, and Michael S. Selig. "New airfoils for small horizontal axis wind turbines." (1998): 108-114. <https://doi.org/10.1115/1.2888052>
- [12] Worasinchai, Supakit, Grant L. Ingram, and Robert G. Dominy. "Effects of wind turbine starting capability on energy yield." *Journal of engineering for gas turbines and power* 134, no. 4 (2012). <https://doi.org/10.1115/1.4004741>

- [13] Abolfazl Pourrajabian, Reza Ebrahimi, and Masoud Mirzaei. "Applying micro scales of horizontal axis wind turbines for operation in low wind speed regions." *Energy conversion and management* 87 (2014): 119-127. <https://doi.org/10.1016/j.enconman.2014.07.003>
- [14] Ali Mostafaeipour. "Economic evaluation of small wind turbine utilization in Kerman, Iran." *Energy Conversion and Management* 73 (2013): 214-225. <https://doi.org/10.1016/j.enconman.2013.04.018>
- [15] Sena, Boni, Sheikh Ahmad Zaki, Hom Bahadur Rijal, Jorge Alfredo Ardila-Rey, Nelidya Md Yusoff, Fitri Yakub, Mohammad Kholid Ridwan, and Firdaus Muhammad-Sukki. "Determinant factors of electricity consumption for a Malaysian household based on a field survey." *Sustainability* 13, no. 2 (2021): 818. <https://doi.org/10.3390/su13020818>
- [16] Majunit, Nurul Izyan, Fazila M. Zawawi, Nur Safwati Mohd Nor, Haslinda Mohamed Kamar, and Nazri Kamsah. "Numerical investigation of vortex formation effect on horizontal axis wind turbine performance in low wind speed condition." *Journal of Advanced Research In Fluid Mechanics And Thermal Sciences* 27, no. 1 (2016): 1-11.
- [17] Canale, Thiago, Kamal Abdel Radi Ismail, and Fátima Aparecida de Morais Lino. "Aerodynamic investigation of alternative airfoils for possible application in small windmills."
- [18] Salih N Akour, Mohammed Al-Heydari, Talha Ahmed, and Kamel Ali Khalil. "Experimental and theoretical investigation of micro wind turbine for low wind speed regions." *Renewable energy* 116 (2018): 215-223. <https://doi.org/10.1016/j.renene.2017.09.076>
- [19] Meng-Hsien Lee, Yui-Chuin Shiah, and Chi-Jeng Bai. "Experiments and numerical simulations of the rotor-blade performance for a small-scale horizontal axis wind turbine." *Journal of Wind Engineering and Industrial Aerodynamics* 149 (2016): 17-29. <https://doi.org/10.1016/j.jweia.2015.12.002>
- [20] Fei-Bin Hsiao, Chi-Jeng Bai, and Wen-Tong Chong. "The performance test of three different horizontal axis wind turbine (HAWT) blade shapes using experimental and numerical methods." *Energies* 6, no. 6 (2013): 2784-2803. <https://doi.org/10.3390/en6062784>
- [21] Anderson, M. B., D. J. Milborrow, and J. N. Ross. "Performance and wake measurements on a 3 m diameter horizontal axis wind turbine. Comparison of theory, wind tunnel and field test data." In *Int. Symp. Wind Energy Syst., Proc. (United Kingdom)*, vol. 2. 1982.
- [22] Wood, David. "Small wind turbines." In *Advances in wind energy conversion technology*, pp. 195-211. Springer, Berlin, Heidelberg, 2011. https://doi.org/10.1007/978-3-540-88258-9_8
- [23] Abdelgalil Eltayesh, Francesco Castellani, Massimiliano Burlando, Magdy Bassily Hanna, AS Huzayyin, Hesham M El-Batsh, and Matteo Becchetti. "Experimental and numerical investigation of the effect of blade number on the aerodynamic performance of a small-scale horizontal axis wind turbine." *Alexandria Engineering Journal* 60, no. 4 (2021): 3931-3944. <https://doi.org/10.1016/j.aej.2021.02.048>
- [24] McCroskey, W. J. *A critical assessment of wind tunnel results for the NACA 0012 airfoil*. No. A-87321. 1987.
- [25] C Eleni Douvi, I Athanasios Tsavalos, and P Dionissios Margaris. "Evaluation of the turbulence models for the simulation of the flow over a National Advisory Committee for Aeronautics (NACA) 0012 airfoil." *Journal of Mechanical Engineering Research* 4, no. 3 (2012): 100-111. <https://doi.org/10.5897/JMER11.074>
- [26] Mohamed A Sayed, Hamdy A Kandil, and Ahmed Shaltot. "Aerodynamic analysis of different wind-turbine-blade profiles using finite-volume method." *Energy conversion and Management* 64 (2012): 541-550. <https://doi.org/10.1016/j.enconman.2012.05.030>
- [27] Bingzheng Dou, Michele Guala, Liping Lei, and Pan Zeng. "Experimental investigation of the performance and wake effect of a small-scale wind turbine in a wind tunnel." *Energy* 166 (2019): 819-833. <https://doi.org/10.1016/j.energy.2018.10.103>
- [28] Shah, H., N. Bhattarai, C. M. Lim, and S. Mathew. "Low Reynolds number airfoil for small horizontal axis wind turbine blades." *Sustainable future energy* (2012).
- [29] Haseeb Shah, Sathyajith Mathew, and Chee Ming Lim. "A novel low Reynolds number airfoil design for small horizontal axis wind turbines." *Wind Engineering* 38, no. 4 (2014): 377-391. <https://doi.org/10.1260/0309-524X.38.4.377>